# A QSAR Study of the Antimalarial Activity of Some Synthetic 1,2,4-Trioxanes[£]

M. Grigorov,[†,‡] J. Weber,[†] J. M. J. Tronchet,[‡] C. W. Jefford,*[,§] W. K. Milhous,[⊥] and D. Maric[||]

Departments of Physical, Pharmaceutical, and Organic Chemistry, University of Geneva, 1211 Geneva 4, Switzerland, Walter Reed Army Institute of Research, Division of Experimental Therapeutics, Washington, D.C. 20307, and Centro Svizzero di Calcolo Scientifico, 6928 Manno, Switzerland

Received July 12, 1996[⊗]

The antimalarial activity of a series of synthetic 1,2,4-trioxanes is correlated with molecular structure by using a pharmacophore search method (CATALYST). The technique is shown to have predictive accuracy and confirms that docking between an active trioxane and the receptor, heme, is the crucial step for drug action.

## INTRODUCTION

Malaria has been known since ancient times and today it is one of the major causes of morbidity and death in the world. Although accurate figures are not available, it is estimated that 2.5 billion people are at risk. Every year some 300 million new clinical cases arise, killing between 2 and 3 million, most of whom are children.[1]

The prevention and cure of malaria depends on a limited number of drugs. Apart from the natural product, quinine, the chief synthetic drugs are quinoline derivatives, such as primaquine, chloroquine, and mefloquine. In addition, simple sulfonamide and pyrimidine derivatives, exemplified by sulfadoxine and pyrimethamine, find use as antimalarial agents by inhibiting the synthesis and reduction of dihydrofolate in the parasite.[2]

Unfortunately, these traditional remedies are no longer adequate. The incidence of malaria by *P. falciparum*, the most dangerous species of parasite, continues to grow, while chloroquine and its congeners are losing their efficacy due to increasing multidrug resistance.[3] Moreover, the sulfadoxine−pyrimethamine combination is no longer recommended because of the risk of severe side effects.[4]

Despite these alarming trends, the discovery that two naturally occurring peroxides, artemisinin (**1**) and yingzhaosu (**2**), possess potent antimalarial activity has opened a new chapter in the chemotherapy of malaria.[5] Since the natural products are complex molecules and embody redundant elements, many structurally simpler 1,2,4-trioxanes have been synthesized and tested for antimalarial activity.[6−8] Thus one of the desiderata for a systematic study of 3D quantitative structure−activity relations (QSAR) is satisfied; namely, a wide range of molecular structures and their complementary activities is available. We now report a QSAR study on some bicyclic and tricyclic 1,2,4-trioxanes with the aim of elucidating the mode of action of this new class of peroxidic antimalarials.

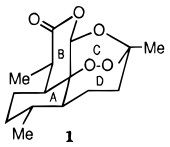


**1**

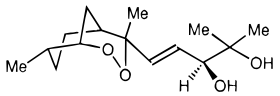


**2**

## MATERIALS AND METHODS

The present study examines synthetic 1,2,4-trioxanes for which were measured either $IC_{90}$ values against the *P. falciparum* W2 (Indochina) and D6 (Sierra Leone) clones *in vitro* or $ED_{90}$ values against *P. berghei N in vivo*.[8,9]

The trioxanes fall into five structural categories. The first category is composed of the tricyclic secoartemisinins (**3**−**6**). Two lack the D ring (**3** and **4**) and the other two the B ring (**5** and **6**). In all four, the lactone ring is missing. However, the remaining carbon skeleton closely resembles

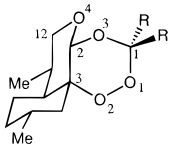


**3** R = Me
**4** R,R = $(CH_2)_4$
(arbitrary numbering)

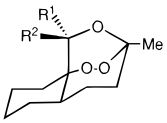


**5** $R^1$ = H, $R^2$ = OMe
**6** $R^1$ = OMe, $R^2$ = H

that of artemisinin (**1**). The second consists of four *cis*-fused cyclohexeno-1,2,4-trioxanes (**7**−**10**) which only vary at the C3 position. All bear *geminal* substituents which are either dimethyl or spirocyclic groups. The third includes the lower homologues, the *cis*-fused cyclopenteno-trioxanes (**11**−**14** and **19**−**21**) bearing the same set of C3-substituents. The

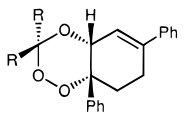


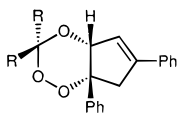


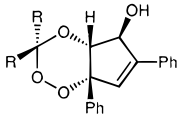


| | | | |
|---|---|---|---|
| **7** | R = Me | **11** | **15** |
| **8** | R,R = $(CH_2)_5$ | **12** | **16** |
| **9** | R,R = $(CH_2)_2O(CH_2)_2$ | **13** | **17** |
| **10** | R,R = $(CH_2)_4$ | **14** | **18** |

fourth category differs slightly from the third in that it is made up of the 5-*exo*-hydroxy, hydroperoxy, and keto derivatives (**15**−**18** and **22**−**25**). A fifth category comprises bridged tricyclic trioxanes in which only the bridgehead substituent varies (**26**−**29**).[10]

[£] Keywords: malaria, artemisinin, heme, 3D-QSAR, CATALYST.
[†] Department of Physical Chemistry, University of Geneva.
[‡] Department of Pharmaceutical Chemistry, University of Geneva.
[§] Department of Organic Chemistry, University of Geneva.
[⊥] Walter Reed Army Institute of Research.
[||] Centro Svizzero di Calcolo Scientifico.
[⊗] Abstract published in *Advance ACS Abstracts,* December 15, 1996.

S0095-2338(96)00116-3 CCC: $14.00 

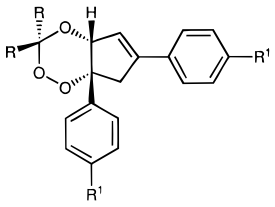

**19** R,R = $(CH_2)_4$, $R^1$ = F
**20** R,R = $(CH_2)_2O(CH_2)_2$, $R^1$ = F
**21** R,R = $(CH_2)_4$, $R^1$ = Pr

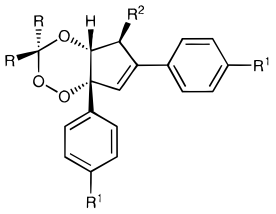

**22** R,R = $(CH_2)_2O(CH_2)_2$, $R^1$ = Me, $R^2$ = OH
**23** R,R = $(CH_2)_2O(CH_2)_2$, $R^1$ = F, $R^2$ = OOH
**24** R,R = $(CH_2)_4$, $R^1$ = Me, $R^2$ = OH
**25** R,R = $(CH_2)_4$, $R^1$ = Me, $R^2$ = O

Trioxanes **3**−**18** and **19**−**25** were chosen for the development of statistical models, hereafter referred to as the training sets. Trioxanes **26**−**29**, referred to as the test-set, were used for assessing the predictive power of the models.

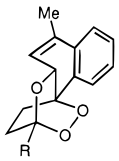

**26** R = H
**27** R = Me
**28** R = Ph
**29** R = Bu

The 3D-QSAR study was performed with the CATALYST package.[11] The geometry of each trioxane was built with the CATALYST builder and optimized by using the generalized CHARMM-like force field[12] implemented in the program. First, the ability of the CHARMM-like force field to accurately reproduce the geometry of the 1,2,4-trioxane ring was verified by comparing the computed parameters with those determined by X-ray crystallography[7] and calculated by an *ab initio* method.[13]

The CATALYST model treats molecular structures as templates consisting of strategically positioned chemical functions that will bind effectively with complementary functions on receptors. The biologically most important binding functions are deduced from a small set of compounds that cover a broad range of activity.[11,14]

Molecular flexibility is taken into account by considering each compound as a collection of conformers representing a different area of conformational space accessible to the molecule within a given energy range. The "best searching procedure" option was applied to select representative conformers in the 0−30 kcal/mol range from the global minimum. Details about the particular way conformational space is sampled by the CATALYST software have already been described.[14−16]

Hypotheses approximating the pharmacophore are described as a set of hydrophobic, hydrogen bond donor, hydrogen bond acceptor, and positively and negatively ionizable sites (PosIon, NegIon) distributed within a 3D space. The features are either point or vector geometrical objects. The directionality of the vector features, namely those associated with hydrogen bonding, is derived from the symmetry, the number of localized lone pairs, and the environment around the ligand atom.[24] The hypotheses are generated using the CatHypo module of CATALYST.[11] The statistical relevance of the various hypotheses so obtained is assessed on the basis of their cost relative to the null hypothesis and their correlation coefficients *R*.[11,17] The hypotheses are then used to estimate the activities of the training set. These activities are derived from those con-

**Table 1.** Selected Experimental and Calculated Bond Lengths, Angles, and Dihedral Angles for Secoartemisinin **3**

| | exptl[a] | *ab initio* (3-21G, HF) | CATALYST force field |
|---|---|---|---|
| **Bond Lengths (Å)** | | | |
| C(1)−O(1) | 1.412 | 1.449 | 1.428 |
| O(1)−O(2) | 1.477 | 1.464 | 1.463 |
| O(2)−C(3) | 1.472 | 1.487 | 1.437 |
| C(3)−C(2) | 1.528 | 1.532 | 1.574 |
| C(2)−O(3) | 1.403 | 1.418 | 1.433 |
| O(3)−C(1) | 1.447 | 1.450 | 1.438 |
| O(4)−C(12) | | 1.419 | 1.430 |
| **Bond Angles (deg)** | | | |
| O(3)−C(1)−O(1) | 109.6 | 107.4 | 111.8 |
| C(1)−O(1)−O(2) | | 107.5 | 112.2 |
| O(1)−O(2)−C(3) | | 111.1 | 113.1 |
| O(2)−C(3)−C(2) | 105.6 | 108.4 | 107.2 |
| C(3)−C(2)−O(3) | 111.3 | 108.0 | 110.4 |
| C(2)−O(3)−C(1) | 116.0 | 116.2 | 116.8 |
| C(2)−O(4)−C(12) | 114.1 | 115.3 | 116.1 |
| **Dihedral Angles (deg)** | | | |
| O(3)−C(1)−O(1)−O(2) | 61.3 | −58.3 | 51.1 |
| C(1)−O(1)−O(2)−C(3) | −71.9 | 67.3 | −59.4 |
| O(1)−O(2)−C(3)−C(2) | 65.9 | −11.2 | 57.5 |
| O(2)−C(3)−C(2)−O(3) | −55.1 | −48.2 | −52.2 |
| C(3)−C(2)−O(3)−C(1) | 48.2 | 59.0 | 49.9 |
| C(2)−O(3)−C(1)−O(1) | −51.5 | −4.4 | −49.6 |
| O(3)−C(2)−O(4)−C(12) | 176.4 | 171.0 | 177.3 |
| C(3)−C(2)−O(4)−C(12) | | 49.8 | 53.7 |

[a] Reference 7.

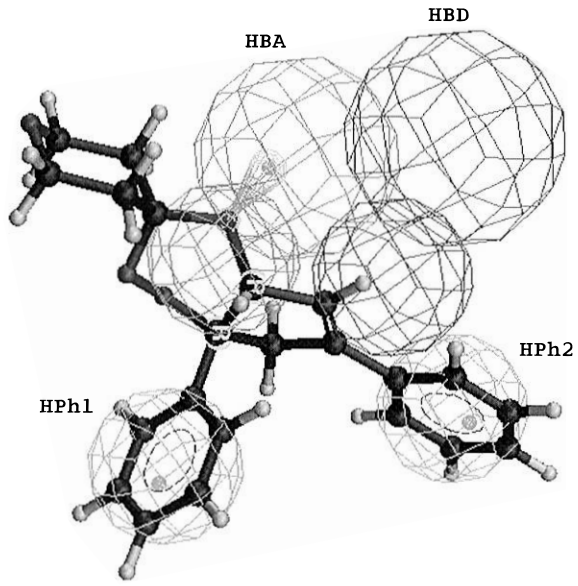


**Figure 1.** Mapping of the most potent member of the W2 training set, **13**, onto the statistically most significant hypothesis.

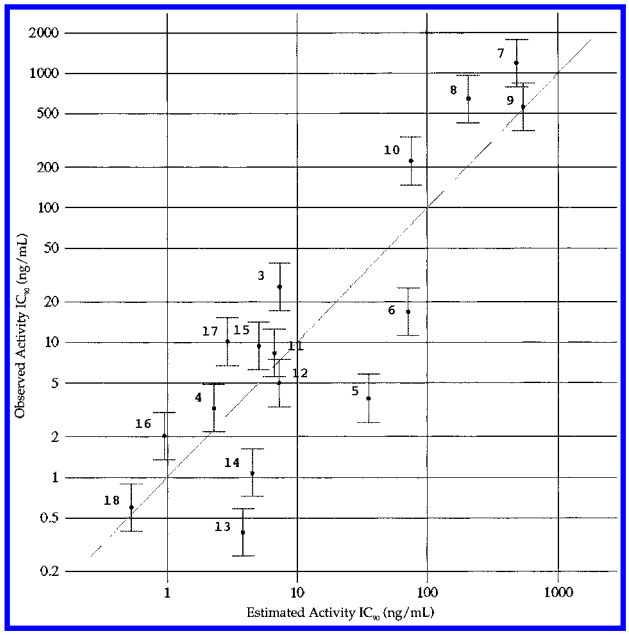


**Figure 2.** Correlation line displaying observed $IC_{90}$ values (ng/mL) *vs* $IC_{90}$ values estimated by using the statistically most significant hypothesis derived from the W2 activities.

formers displaying the smallest root-mean square (RMS) deviations when projected onto the hypothesis.[11]

## RESULTS AND DISCUSSION

**Evaluation of the Capability of the Molecular Force Field as Implemented in CATALYST To Reproduce the Geometry of the 1,2,4-Trioxane Ring.** The tricyclic secoartemisin **3** was taken as representative of the training set. The calculated bond lengths compare well with those determined by X-ray (Table 1). The bond angles, both calculated and experimental, are also in close agreement. The CATALYST force field does better than the *ab initio* method in predicting the dihedral angles and calculates reliably the conformations of the molecules in question. In general, the force field method is as good as the *ab initio* method. It can therefore be concluded that the implemented CHARMM-like force field accurately reproduces the geometry of the trioxane ring.

**Table 2.** Observed *in vitro* ($IC_{90}$) and *in vivo* ($ED_{90}$) Activities of Some 1,2,4-Trioxanes

| compd[a] | *P. falciparum* Indo-China W2 clone $IC_{90}$, ng/mL | *P. falciparum* Sierra Leone D6 clone $IC_{90}$, ng/mL |
|---|---|---|
| **1** | 1.1[b] | 2.3[b] |
| **3** | 25.8 | 59.8 |
| **4** | 3.3 | 30.4 |
| **5** | 3.8 | 11.5 |
| **6** | 16.9 | 875.0 |
| **7** | 1184.0 | 1260.0 |
| **8** | 643.0 | 2585.0 |
| **9** | 560.0 | 1407.0 |
| **10** | 223.0 | 243.0 |
| **11** | 8.4 | 19.3 |
| **12** | 5.0 | 12.2 |
| **13** | 0.4 | 12.5 |
| **14** | 1.1 | 2.3 |
| **15** | 9.4 | 10.2 |
| **16** | 2.0 | 5.0 |
| **17** | 10.2 | 20.2 |
| **18** | 0.6 | 10.6 |
| **26** | inactive | inactive |
| **27** | 1135.0 | 662.0 |
| **28** | 568.0 | 488.0 |
| **29** | 30.0 | 35.0 |

| compd[a] | *P. berghei* N, $ED_{90}$, mg/kg × 4, s.c. |
|---|---|
| **19** | 6.8 |
| **20** | 19.5 |
| **21** | 22.5 |
| **22** | 17.0 |
| **23** | 13.2 |
| **24** | 15.0 |
| **25** | 16.0 |

[a] For all compounds except **26**−**29**, data obtained from refs 8 and 9. New data for **26**−**29**. [b] $IC_{50}$ values used as $IC_{90}$, not available.

**Assessment of 3D-QSAR for *in vitro* Antimalarial Activity.** A search for the pharmacophore was undertaken

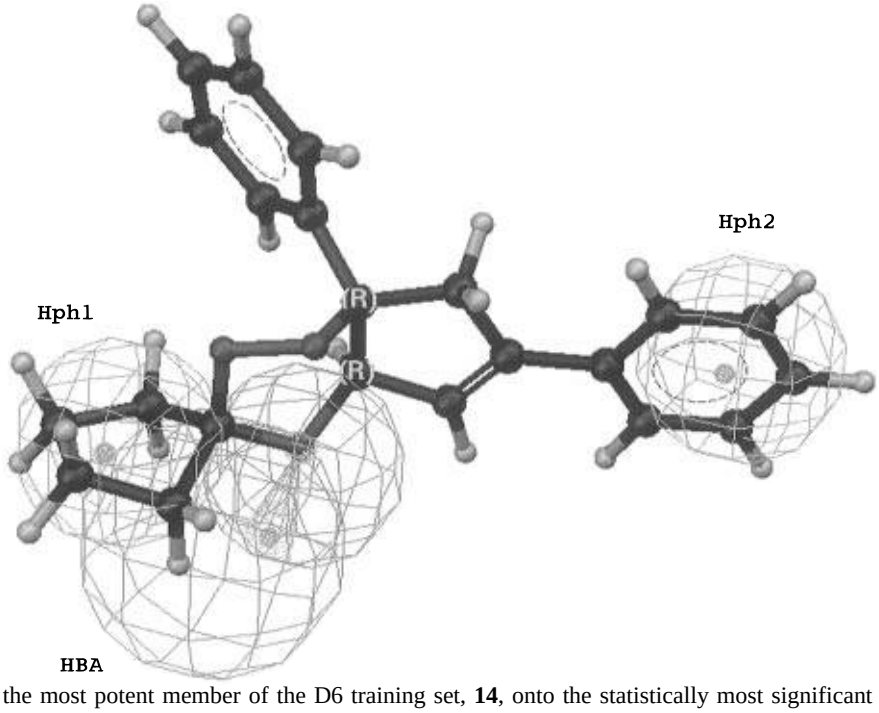


**Figure 3.** Mapping of the most potent member of the D6 training set, **14**, onto the statistically most significant hypothesis.

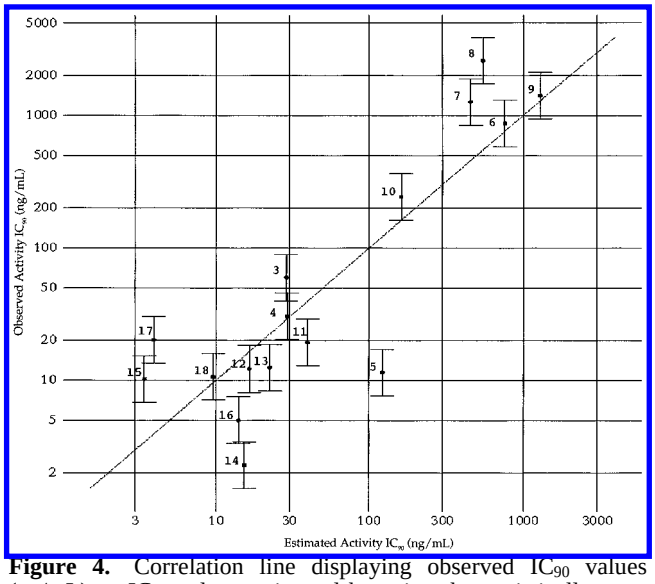


**Figure 4.** Correlation line displaying observed $IC_{90}$ values (ng/mL) *vs* $IC_{90}$ values estimated by using the statistically most significant hypothesis derived from the D6 activities.

by setting the default parameters of CATALYST to the following values: function weight 0.302, mapping coefficient 0, resolution 297 pm, and activity uncertainty 3. Within the CATALYST paradigm, an uncertainty $\delta$ in the biological activity means that the activity is situated somewhere in the interval from activity/$\delta$ to activity $\times$ $\delta$. Although it is easier to search for the pharmacophore by using rigid structures in the training set, we decided instead to examine *cis*-fused molecules since they offer a broad range of conformations thereby permitting the optimal pharmacophore to be defined. From a consideration of the chemical structure of the molecules in the *in vitro* training set, hydrophobic sites (HPh), hydrogen bond acceptors (HBA), hydrogen bond donors (HBD), positively and negatively ionizable sites (PosIon), and negatively ionizable sites (NegIon) were selected as being the features best suited to explain the biological activity. These features were then taken for the automatic generation of hypotheses. It should be noted that in the CATALYST program there is no feature corresponding to the peroxide bond as such.

First, we decided to take the observed *in vitro* activities, namely the $IC_{90}$ values, of **3**−**18** against the W2 Indochina clone in order to procure a model for the pharmacophore (Table 2). It was found that only four of the five features are embodied in the statistically most significant hypothesis (cost = 120.616, cost of the null hypothesis = 324.974, $R$ = 0.876). The most potent member of the *in vitro* training set, **13**, maps well with the hypothesis (Figure 1). The two phenyl groups overlap with the hydrophobic features, whereas the nonperoxidic oxygen atom serves as a H-bond acceptor. However, the HBD feature finds no counterpart on the molecule. This optimal hypothesis was used to estimate the activities of all members (**3**−**18**) in the training set. The correlation between observed and estimated W2 activities is satisfactory (Figure 2).

The preceding procedure was repeated for the *in vitro* activities of **3**−**18** against the D6 Sierra Leone clone (Table 2). The most active member **14** maps closely with the new hypothesis (cost = 116.462, cost of the null hypothesis = 267.628, $R$ = 0.853), which this time is made up of only three features (Figure 3). The spirocyclic group and one of the phenyl groups overlay the hydrophobic features. As before, the nonperoxidic oxygen atom is the focus of the HBA feature. On applying the hypothesis to the set, the observed and estimated D6 activities show a good correlation (Figure 4).

**Assessment of 3D-QSAR for *in vivo* Antimalarial Activity.** A hypothesis for the pharmacophore responsible for *in vivo* antimalarial activity was computed by setting the default parameters of CATALYST to the following values: function weight 0.302, mapping coefficient 0, resolution 297 pm, and activity uncertainty 3. As the molecules in the training set, **19**−**25**, belong to the same structural categories as **7**−**18**, the same five features were chosen. These features were automatically processed as before to generate hypotheses. The activities exhibited by the training set against *P. berghei*, the $ED_{90}$ values, were taken for constructing the relevant pharmacophore (Table 2). The most active member, **19**, maps closely with the statistically most significant hypothesis, which again is characterized by just three features

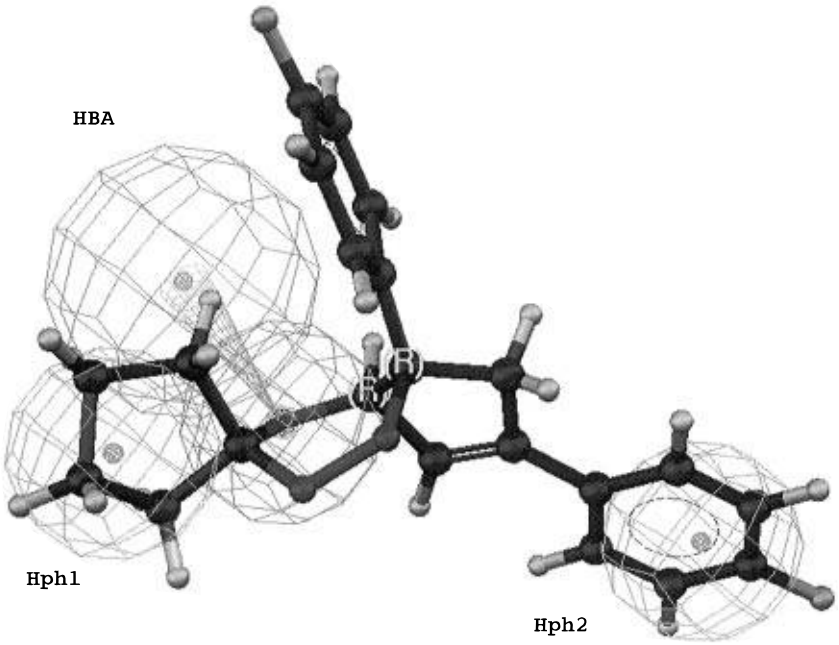


**Figure 5.** Mapping of the most potent member of the *P. berghei* training set, **19**, onto the statistically most significant hypothesis.

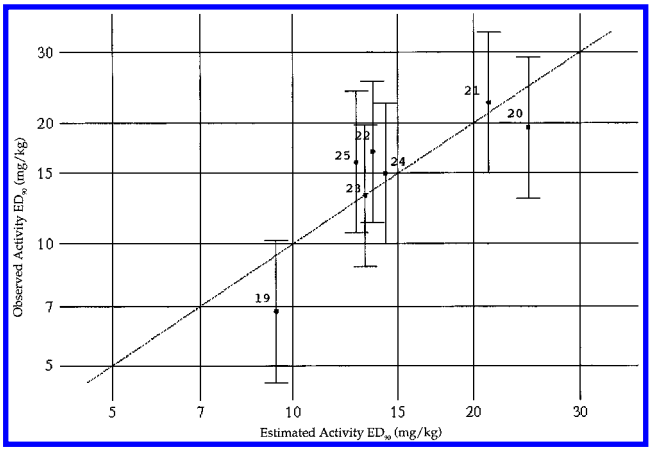


**Figure 6.** Correlation line displaying observed $ED_{90}$ values (mg/kg) *vs* $ED_{90}$ values estimated by using the statistically most significant hypothesis derived from the *in vivo* antimalarial activities.

(Figure 5). The pair of hydrophobic features overlap neatly with the spirocyclic and phenyl groups, respectively, and the hydrogen bonding acceptor is disposed over the O(4)-atom. The hypothesis turns out to be an accurate measure for the whole training set as attested by the reasonably good correlation between observed and estimated activities (cost = 5.230, cost of the null hypothesis = 24.847, $R = 0.839$) (Figure 6).

**Comparison of the *in vitro* and *in vivo* Hypotheses.** Inspection of the *in vitro* and *in vivo* hypotheses reveals that they share the same three features and are very nearly superimposable. This coincidence is not surprising because the training sets comprise similar, conformationally mobile *cis*-fused bicyclic structures.

**Validation of the Hypothesis.** The hypothesis for antimalarial activity derived from the *cis*-fused cyclopenteno-1,2,4-trioxanes in the D6 training set was next tested on the trioxanes **26**−**29**. These molecules, the test set, although trioxanes, are radically different from the others. They are rigid, bridged, bicyclic structures containing a spirocyclic dihydronaphthalene element.[10] Conformers and their energies for **26**−**29** were generated according to the previously described methodology. The respective activities were then derived for the conformer which fits the best with the hypothesis (Table 3). The predicted activities are in the right order and parallel the values actually observed (Table 2).

**Receptor-Drug Interaction.** Recent studies have demonstrated that the receptor for artemisinin is heme which is the byproduct of the degradation of hemoglobin ingested by the intraerythrocytic parasite.[18−21] The present studies on synthetic trioxanes demonstrate that two hydrophobic sites and a hydrogen acceptor site located on the drug seem to be essential for antimalarial activity. By analogy, heme would be expected to interact with an active synthetic trioxane by deploying the counterparts of the features of the hypothesis. While heme has several hydrophobic sites available for binding, the counterpart for the hydrogen bond acceptor site is more problematical. The only sites accessible are the pendent carboxylic groups. As the latter are ionized in solution, we suggest that the juxtaposition of a weakly bound

**Table 3.** Energies of Conformers of Trioxanes **26**−**29** and Their Estimated and Observed Antimalarial Activities *in vitro*

| compd | no. of conformers generated | first conformer with nonzero energy (kcal/mol) | energy of the conformer which maps the best on the hypothesis (kcal/mol) | $IC_{90}$ est. (ng/mL) | $IC_{90}$ obsd (ng/mL) | |
|---|---|---|---|---|---|---|
| | | | | | W2 | D6 |
| **26** | 5 | 20.396 | 24.741 | 1300 | inactive | inactive |
| **27** | 5 | 22.488 | 29.437 | 1300 | 1135 | 662 |
| **28** | 6 | 17.060 | 29.018 | 690 | 568 | 488 |
| **29** | 17 | 2.581 | 17.597 | 53 | 30 | 35 |

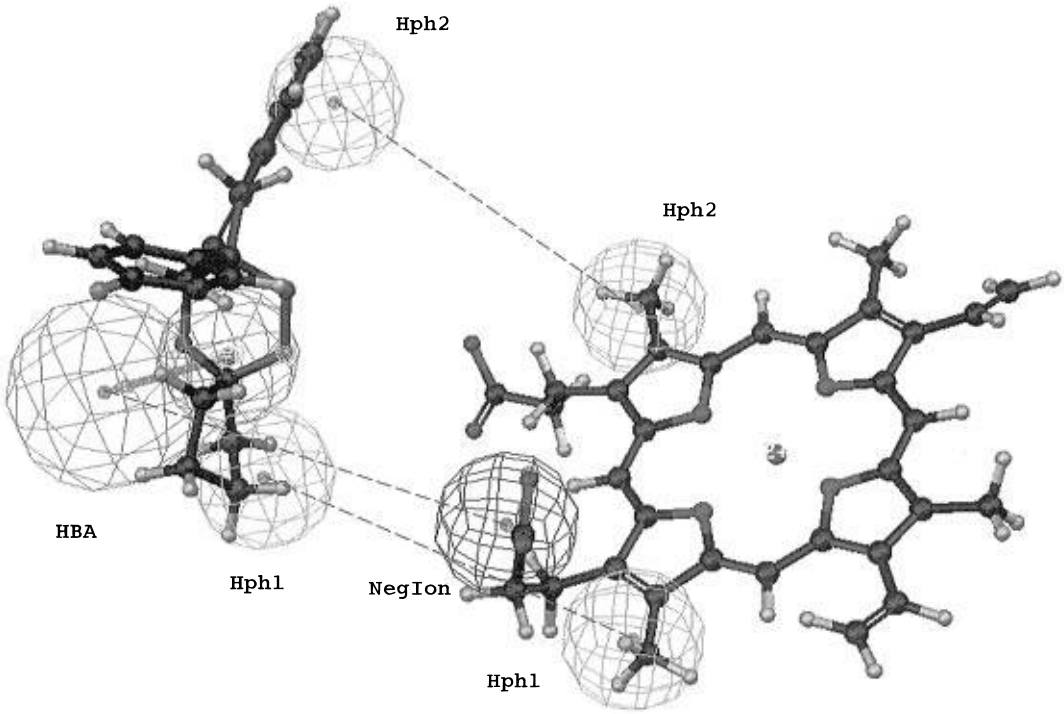


**Figure 7.** Binding sites on **19** and their counterparts on the receptor, heme, responsible for forming a stable drug-receptor complex.

**Table 4.** Energies of Conformers of **1** and **30**−**32** and Their Predicted Antimalarial Activities *in vitro*

| compd. | no. of conformers generated | first conformer with nonzero energy (kcal/mol) | energy of the conformer which maps the best on the hypothesis (kcal/mol) | $IC_{90}$ est. (ng/mL) |
|---|---|---|---|---|
| **1** | 3 | 0.617 | 0.000 | 8.7 |
| **30** | 5 | 14.772 | 19.596 | 110 |
| **31** | 4 | 8.785 | 8.785 | 1100 |
| **32** | 4 | 0.637 | 1.745 | 1040 |

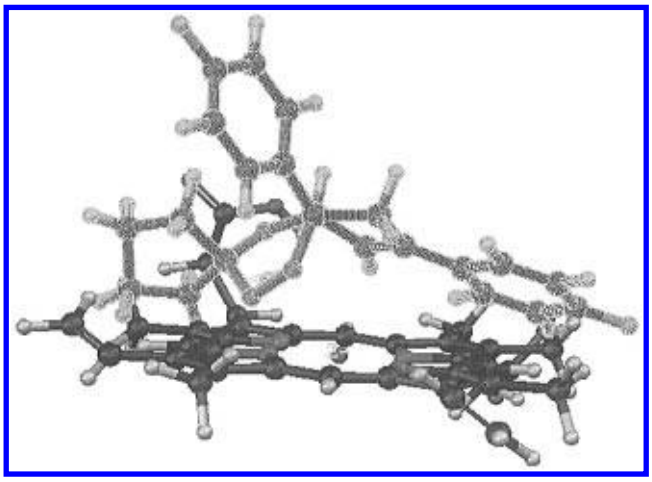

**Figure 8.** Perspective view of the complex between **19** and heme.

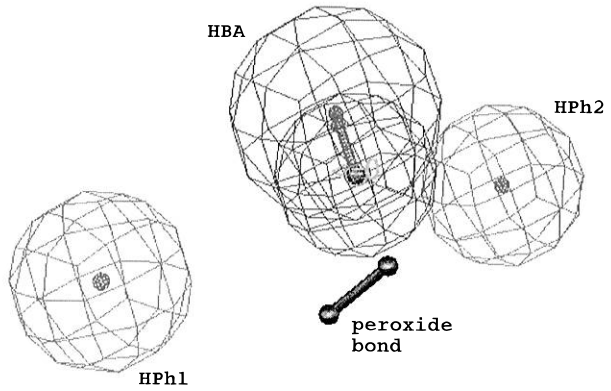


**Figure 9.** Query for searching the NCI database. The essential elements, positioned in 3D space for a candidate having high antimalarial activity.

molecule of solvent water will create the appropriate H-bond donor.

The next stage of the analysis of the drug-receptor interaction is to evaluate the constraints on the positions of the two hydrophobic sites and the hydrogen bond donor site located on heme. These positions must correspond to those of the counterparts on the drug molecule, designated as **19** for the present purposes. Consequently, the CHARMM-like CATALYST force field, appropriately parameterized for heme derivatives,[22] was used to generate heme conformers according to the already described procedure. Of the seven conformers so generated a fit with the counterparts of the sites present on **19** was sought by taking into account the distance constraints. In principle, as heme and **19** possess several lipophilic sites many pairings are possible. However, the smallest RMS deviations between complementary features were obtained when the conformer lying at 4.239 kcal/mol above the most stable conformer of heme was superimposed on the hypothesis for the antimalarial activity of **19** (Figure 7).

The resulting complex reveals that one of the peroxidic oxygen atoms lies extremely close to the ferrous ion (1.2−1.5 Å) (Figure 8). Such close contact is not to be construed as bond formation but merely as an index of contiguity. This contiguity is of paramount importance for parasiticidal action which depends on the efficiency of electron transfer from ferrous ion toward the peroxide bond.[19−21] It is also seen that a phenyl group of **19** lies face-to-face over one of the pyrrole rings of heme. Thus, $\pi-\pi$ stacking may be important for stabilizing the drug-receptor complex.

**Searching the NCI Database for New Antimalarial Leads.** We have performed a search for new antimalarial candidates in the NCI drugs database[23] delivered in a special

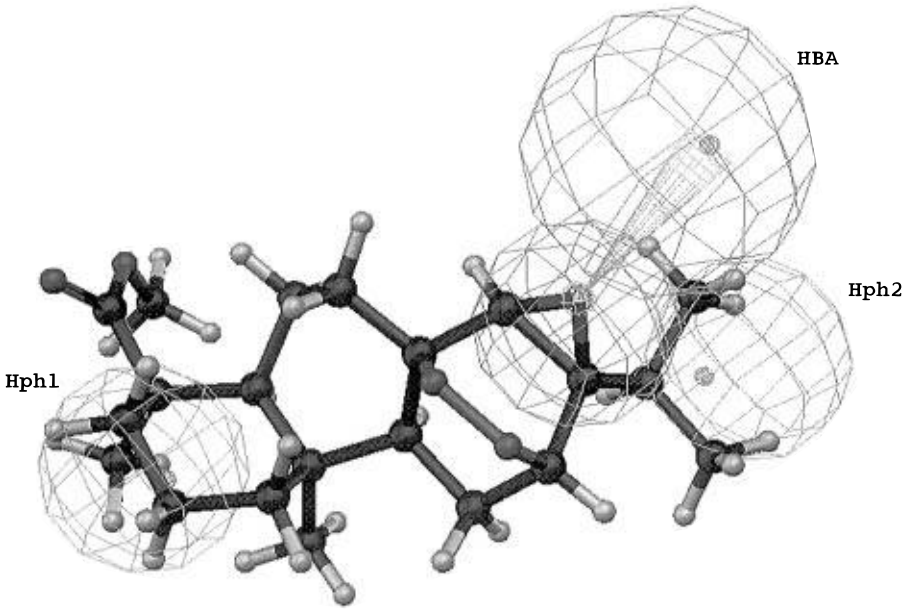


**Figure 10.** Mapping of **30** onto the hypothesis derived from the *in vitro* antimalarial activities.

format with the CATALYST software. In this format, each drug is represented by a limited set of conformations thereby permitting conformational flexibility to be included during the database search. The CATALYST methodology for searching databases through queries has been described.[24] A database query was formulated by superimposing the *in vivo* hypothesis and a conformer of **14**. All atoms were eliminated from the molecular framework except the peroxide element. The final query thus contains three position constraints for the sites of the receptor-drug interaction together with the peroxide bond (Figure 9). The database search led to the discovery of four compounds that have a high overlap with the query just described. As expected, one was artemisinin (**1**). The other three compounds (**30**−**32**) are derivatives of abietic acid.[25−27] Their antimalarial activities were estimated (Table 4). Artemisinin (**1**) is predicted to have an activity which is about four times smaller than that actually observed. In comparison, the peroxides **31** and **32** are essentially inactive as the values predicted are some hundred times less than that of **1**. However, the peroxide **30** shows promise, probably on account of the locus provided for hydrogen bonding (Figure 10).

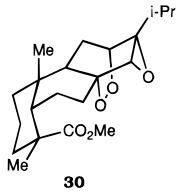


**30**

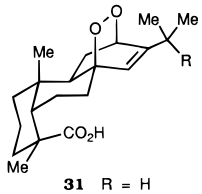


**31** R = H
**32** R = OOH

## CONCLUSION

The present work shows how a set of antimalarial activities of various 1,2,4-trioxanes may be treated statistically to uncover the molecular characteristics which are essential for high activity. These characteristics are expressed as chemical features disposed in three-dimensional space and are collectively termed a hypothesis. Two hydrophobic features and hydrogen bonding are the minimum components of an effective antimalarial hypothesis. The validity of the hypothesis extends to trioxanes which are structurally different from those of the training set. The counterpart of such hypotheses is also shown to account for the interaction, or docking, between the receptor, heme, and an active trioxane drug. The peroxide bond of the trioxane is found to lie close to the central ferrous atom of heme thereby fulfilling a criterion for parasiticidal action.[18−21]

## ACKNOWLEDGMENT

This work was generously supported by the Helmut Horten Foundation, the Swiss Federal Office for Public Health, and the Swiss National Science Foundation (Grant Nos. 3139-037156, 20-37626.93, 20-43552.95, and 20-41830.94). The CATALYST Software was made available through a University Research partnership.

## REFERENCES AND NOTES

(1) *T.D.R. News* **1994**, *46*, 5.
(2) *Chemotherapy of Malaria*, 2nd ed.; Bruce-Chwatt, L. J., Ed.; W.H.O.: Geneva, 1981.
(3) Peters, W. *Chemotherapy and Drug Resistance in Malaria*, 2nd ed.; Academic Press: London, 1987. Wernsdorfer, W. H. *Parasitology Today* **1991**, *7*, 297−231.
(4) Miller, K. D.; Lobel, H. O.; Satriale, R. F.; Kuritsky, J. N.; Stern, R.; Campbell, C. C. *Am. J. Trop. Med. Hyg.* **1986**, *5*, 451−458.
(5) Klayman, D. L. *Science* **1985**, *228*, 1049−1055. Butler, A. R.; Wu, Y. L. *Chem. Soc. Rev.* **1992**, 85−90. Shen, C. C.; Zhuang, L. G. *Med. Res. Rev.* **1984**, *4*, 47−86.
(6) Jefford, C. W.; Velarde, J. A.; Bernardinelli, G.; Bray, D. H.; Warhurst, D. C.; Milhous, W. K. *Helv. Chim. Acta* **1993**, *76*, 2775−2788.
(7) Jefford, C. W.; Wang, Y.; Bernardinelli, G. *Helv. Chim. Acta* **1988**, *71*, 2042−2052.
(8) Jefford, C. W.; Misra, D.; Rossier, J.-C.; Kalamaprija, P.; Burger, U.; Mareda, J.; Bernardinelli, G.; Peters, W.; Robinson, B. L.; Milhous, W. K.; Zhang, F.; Gosser, J.; Meshnick, S. R., Jr. In *Perspectives in Medicinal Chemistry*; Testa, B., Kyburz, E., Fuhrer, W., Giger, R., Eds.; VCH Publishers: Amsterdam, 1992; Vol. 25, Chapter 29, pp 459−472.
(9) Peters, W.; Robinson, B. L.; Rossier, J.-C.; Misra, D.; Jefford, C. W. *Ann. Trop. Med. Parasitol.* **1993**, *87*, 9−16. Peters, W.; Robinson, B. L.; Tovey, G.; Rossier, J.-C.; Jefford, C. W. *Ann. Trop. Med. Parasitol.* **1993**, *87*, 111−123.
(10) Jefford, C. W.; Favarger, F.; Ferro, S.; Chambaz, D.; Bringhen, A.; Bernardinelli, G.; Boukouvalas, J. *Helv. Chim. Acta* **1986**, *69*, 1778−1786.
(11) CATALYST Version 2.0 software; Molecular Simulations Inc.: Burlington, MA, 1993.
(12) Brooks, B. R.; Brucolleri, R. E.; Olafson, B. D.; States, D. J.; Swaminathan, S.; Karplus, M. *J. Comput. Chem.* **1983**, *4*, 187−217.
(13) Bernardinelli, G.; Jefford, C. W.; Maric, D.; Thomson, C.; Weber, J. *Int. J. Quant. Chem.* **1994**, *21*, 117−131.
(14) Sprague, P. In *Perspectives in Drug Discovery and Design*; Anderson, P. S.; Kenyon, G. L., Marshall, G. R., Müller, K., Eds.; ESCOM: Leiden, 1995; Vol. 3, Chapter 1, pp 1−20.
(15) Smellie, A.; Kahn, S. D.; Teig, S. L. *J. Chem. Inf. Comput. Sci.* **1995**, *35*, 285−294.
(16) Smellie, A.; Kahn, S. D.; Teig, S. L. *J. Chem. Inf. Comput. Sci.* **1995**, *35*, 295−304.
(17) Fisher, R. *The Design of Experiments*; Hafner Publishing: New York, 1966; Chapter 2.
(18) Zhang, F.; Gosser, D. K.; Meshnick, S. R., Jr. *Biochem. Pharm.* **1992**, *43*, 1805−1809.
(19) Meshnick, S. R., Jr.; Jefford, C. W.; Posner, G. H.; Avery, M. A.; Peters, W. *Parasitology Today* **1996**, *12*, 79−82.
(20) Jefford, C. W.; Kohmoto, S.; Jaggi, D.; Timári, G.; Rossier, J.-C.; Rudaz, M.; Barbuzzi, O.; Gérard, D.; Burger, U.; Kamalaprija, P.; Mareda, J.; Bernardinelli, G.; Manzanares, I.; Canfield, C. J.; Fleck, S. L.; Robinson, B. L.; Peters, W. *Helv. Chim. Acta* **1995**, *78*, 647−662.
(21) Jefford, C. W.; Vicente, M. G. H.; Jacquier, Y.; Favarger, F.; Mareda, J.; Millasson-Schmidt, P.; Brunner, G.; Burger, U. *Helv. Chim. Acta* **1996**, *79*, 1475−1487.
(22) Dr. O. Schaad, Department of Biochemistry, University of Geneva, personal communication.
(23) NCI drugs database, version 31; Molecular Simulations Inc.: January 1994.
(24) Greene, J.; Kahn, S. D.; Savoj, H.; Sprague, P.; Teig, S. *J. Chem. Inf. Comput. Sci.* **1994**, *34*, 1297−1308.
(25) Leibuyk, T. V.; Svetsov, S. A.; Raldugin, V. A. *Khim. Prir. Soed.* **1990**, *4*, 556−557.
(26) Herz, W.; Ligon, R. C.; Turner, J. A.; Blount, J. F. *J. Org. Chem.* **1977**, *42*, 1885−1894.
(27) Schuller, W. H.; Lawrence, R. V. US Patent US3463769-690826.

CI9601168